Loss of Bardet–Biedl syndrome proteins alters the morphology and function of motile cilia in airway epithelia

Alok S. Shah*, Sara L. Farmen*, Thomas O. Moninger*, Thomas R. Businga*, Michael P. Andrews†, Kevin Bugge†, Charles C. Searby†, Darryl Nishimura†, Kim A. Brogden‡§, Joel N. Kline*, Val C. Sheffield†¶, and Michael J. Welsh*¶‖**

Departments of *Internal Medicine, †Pediatrics, and ‖Molecular Physiology and Biophysics, and ¶Howard Hughes Medical Institute, Roy J. and Lucille A. Carver College of Medicine, and ‡Department of Periodontics and §Dows Institute for Dental Research, College of Dentistry, University of Iowa, Iowa City, IA 52242

Contributed by Michael J. Welsh, December 28, 2007 (sent for review December 18, 2007)

Mutations in a group of genes that contribute to ciliary function cause Bardet–Biedl syndrome (BBS). Most studies of BBS have focused on primary, sensory cilia. Here, we asked whether loss of BBS proteins would also affect motile cilia lining the respiratory tract. We found that BBS genes were expressed in human airway epithelia, and BBS2 and BBS4 localized to cellular structures associated with motile cilia. Although BBS proteins were not required for ciliogenesis, their loss caused structural defects in a fraction of cilia covering mouse airway epithelia. The most common abnormality was bulges filled with vesicles near the tips of cilia. We discovered this same misshapen appearance in airway cilia from *Bbs1*, *Bbs2*, *Bbs4*, and *Bbs6* mutant mice. The structural abnormalities were accompanied by functional defects; ciliary beat frequency was reduced in *Bbs* mutant mice. Previous reports suggested BBS might increase the incidence of asthma. However, compared with wild-type controls, neither airway hyperresponsiveness nor inflammation increased in *Bbs2*$^{-/-}$ or *Bbs4*$^{-/-}$ mice immunized with ovalbumin. Instead, these animals were partially protected from airway hyperresponsiveness. These results emphasize the role of BBS proteins in both the structure and function of motile cilia. They also invite additional scrutiny of motile cilia dysfunction in patients with this disease.

asthma | basal body

Bardet–Biedl syndrome (BBS) is a rare, pleiotropic, autosomal recessive disorder (1, 2). Its diverse manifestations include obesity, hypertension, retinopathy, polydactyly, hypogenitalism, renal abnormalities, and developmental delay. In addition, patients with BBS may have an increased incidence of asthma; some reports suggest that 25–28% of patients have asthma (2, 3). The association with asthma led us to investigate the airways in BBS.

Although mutations in any of 12 different genes (*BBS1-12*) can cause BBS, the BBS proteins show little structural similarity (1, 4, 5). Thus, until recently, it has seemed puzzling that mutations in these 12 unrelated genes would all produce the same clinical BBS phenotype. Recent observations have provided some insight. (*i*) *BBS* genes appear to be highly conserved in organisms with cilia but not in organisms without cilia (6–8). (*ii*) Studies of mice with targeted mutation of *Bbs* genes (9–12) and zebrafish with knockdown of *Bbs* genes (13) indicate a role for BBS proteins in cilia formation and function. (*iii*) BBS proteins are located in the neighborhood of primary cilia, including the basal body, the ciliary axoneme, and the pericentriolar region (14–16). (*iv*) Biochemical studies found a protein complex, the BBSome, containing seven BBS proteins localized to centrioles and primary cilia (4). In combination, these observations suggested that BBS is caused by defects in cilia structure and/or function.

Cilia contain a central microtubule arrangement and an intraflagellar transport (IFT) system (17–19). In general, they are classified as primary or motile cilia. Although there are exceptions (19), primary cilia contain microtubules arranged as doublets in a 9 + 0 pattern. These cilia are usually immotile and serve as sensory organelles; examples include cilia in photoreceptors, olfactory cells, and renal collecting duct cells. Motile cilia also have nine microtubule doublets. In addition, most contain two central singlet microtubules, producing a 9 + 2 pattern, plus outer dynein arms and radial spokes. Motile cilia serve a mechanical function, beating regularly; examples include cilia on respiratory epithelia, oviduct, and brain ventricles.

Most studies of BBS have focused on primary cilia. However, BBS can also involve motile cilia as demonstrated by the lack of sperm flagella in *Bbs1*, *Bbs2*, *Bbs4*, and *Bbs6* mutant mice (9–12). Yet little is known about whether loss of BBS proteins affects other motile cilia, such as those covering airway epithelia. Previous studies of mice with mutated *BBS* genes have reported that respiratory cilia were present and were grossly normal (9, 10, 20), although the morphology has not been examined in depth.

Given that BBS affects primary cilia and that primary and motile cilia contain many of the same components, we hypothesized that loss of BBS proteins might alter the structure or function of motile cilia on airway epithelia.

Results

Human Airway Epithelia Express *Bbs* Genes. We used primary cultures of human and mouse airway epithelia grown at the air–liquid interface (21, 22). After 2 weeks, the epithelia develop a differentiated morphology with ciliated, goblet, basal, and other columnar cells. Microarray expression analysis using mRNA isolated from these human epithelia revealed that all 12 *Bbs* genes were expressed [supporting information (SI) Fig. 7]. These results are consistent with reports that lung expresses *BBS2*, *BBS4*, and *BBS6* (9, 10, 14, 16, 23). In subsequent studies, we focused on BBS proteins that were present in the BBSome and for which we had gene-targeted mice.

BBS2 and BBS4 Localize to Cilia-Related Structures and the Pericentriolar Region in Human Airway Epithelia. We attempted to immunolocalize BBS2 and BBS4. However, we could not be confident

Author contributions: A.S.S., S.L.F., J.N.K., V.C.S., and M.J.W. designed research; A.S.S., S.L.F., T.O.M., T.R.B., and K.A.B. performed research; A.S.S., M.P.A., K.B., C.C.S., D.N., and V.C.S. contributed new reagents/analytic tools; A.S.S., T.O.M., T.R.B., K.A.B., J.N.K., V.C.S., and M.J.W. analyzed data; and A.S.S., V.C.S., and M.J.W. wrote the paper.

The authors declare no conflict of interest.

Freely available online through the PNAS open access option.

**To whom correspondence should be addressed at: Howard Hughes Medical Institute, Department of Internal Medicine, 500 EMRB, Roy J. and Lucille A. Carver College of Medicine, University of Iowa, Iowa City, IA 52242. E-mail: michael-welsh@uiowa.edu.

This article contains supporting information online at www.pnas.org/cgi/content/full/0712327105/DC1.

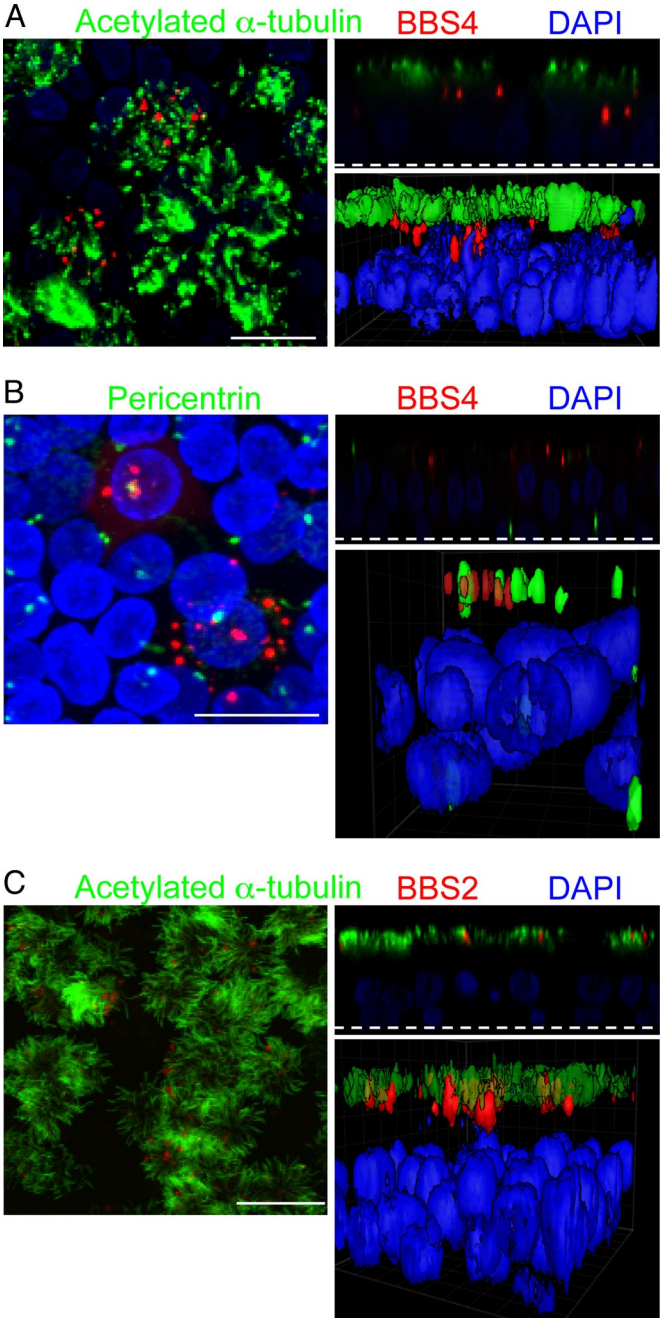

Fig. 1. BBS4 and BBS2 localized to cilia and related structures in primary cultures of differentiated human airway epithelia. Airway epithelia were infected with Ad-3xFlag-tagged-BBS4 (*A* and *B*) or BBS2 (*C*) and immunostained 28 h later. Each image shows a stack of X-Y confocal images on the left, a single X-Z image in the upper right (the dashed line indicates the top of the filter on which epithelia grew), and a 3D surface projection in the lower right. (*A*) BBS4 (red) localized in multiple puncta beneath the cilia in the area of the basal body. Acetylated α-tubulin (green) is a marker of cilia (45). Nuclei were stained with DAPI (blue). (*B*) BBS4 (red) localized adjacent to or with pericentrin (green). Pericentrin staining occurred at the basal bodies in the apical portion of ciliated cells and near the nucleus of basal cells in centrioles (24). (*C*) BBS2 (red) localized in the region of cilia (acetylated α-tubulin, green) and the basal body. Control epithelia treated with secondary antibodies showed no staining (data not shown). (Scale bars: 10 μm.)

of specific immunostaining because *Bbs2*$^{-/-}$ and *Bbs4*$^{-/-}$ mouse epithelia also showed some staining. Therefore, we used adenovirus vectors to express 3xFLAG-tagged human BBS proteins

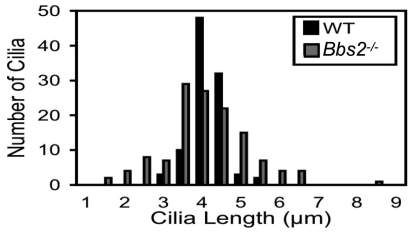

Fig. 2. Loss of BBS2 changed the distribution of cilia length. Cilia length was measured by using light microscopy of H&E sections. *Bbs2*$^{-/-}$ and wild-type cilia showed the same average length: 4.1 μm. However, *Bbs2*$^{-/-}$ cilia exhibited a greater variation in length; variance for wild-type cilia (0.20) differed from *Bbs2*$^{-/-}$ cilia (1.22); $P < 0.001$, Levene test.

in human airway epithelia. To reduce artifacts due to BBS protein overexpression, we examined cells as soon as the recombinant protein could be detected. As a control for BBS protein localization, we compared the localization of the FLAG-tagged BBS4 to that of BBS4 reported earlier. Kim *et al.* (16) localized endogenous BBS4 adjacent to the centriole in Cos-7 cells; we obtained similar results with the tagged BBS4 in Cos-7 and HeLa cells (SI Fig. 8).

In airway epithelia, we found punctate BBS4 immunostaining with multiple spots per ciliated cell (Fig. 1*A*). Because not all of the cells were infected by the vector, only some show the BBS proteins. BBS4 localized beneath the cilia, which were stained with acetylated α-tubulin. Three-dimensional surface projections and X-Z scans confirmed the presence of BBS4 below cilia, at the position where we would expect to find basal bodies. As an additional test of BBS4 localization to basal bodies, we coimmunostained with pericentrin, which is known to localize to basal bodies and centrioles (24). BBS4 sat adjacent to and with pericentrin (Fig. 1*B*).

BBS2 immunostaining showed a related pattern, with multiple puncta in ciliated cells (Fig. 1*C*). However, it localized higher in the cell than BBS4, often colocalizing with the acetylated α-tubulin.

Loss of BBS Alters Ciliary Morphology. Lungs of *Bbs2*$^{-/-}$ and *Bbs4*$^{-/-}$ mice had a normal gross morphology and morphometric analysis (SI Fig. 9). We also measured the length of cilia covering the surface of tracheal epithelia (Fig. 2). Although wild-type and *Bbs2*$^{-/-}$ cilia had the same average length, there was greater variation in the mutant epithelia. Interestingly, *Chlamydomonas* IFT-mutant flagella and renal cilia in *Bbs4*$^{-/-}$ mice produce both long and short cilia (25, 26).

We used scanning electron microscopy (SEM) to better assess ciliary morphology in *Bbs2*, *Bbs4*, and *Bbs6* null and *Bbs1-M390R* mutant mice. Consistent with light-level microscopy and previous reports, cilia were present on airway epithelia, indicating that these BBS proteins are not required for ciliogenesis (Fig. 3 *A–F*). However, in all of the mutant strains, some of the cilia displayed morphologic abnormalities. The shapes varied and included two main alterations. The most common defect was a dilated or enlarged appearance, usually at the cilia tip, but sometimes along the ciliary shaft. These cilia appeared cup-shaped, paddle-shaped, or bulging (Fig. 3 *B* and *C*). Less frequently, the distal ends of cilia appeared to have sprouted one or more short stubby fingers (Fig. 3*B*). The morphologic changes were not the result of culturing epithelia, because in airway epithelia prepared directly from the mice, we observed similar changes, albeit with a lower frequency (Fig. 3 *D–F*). Moreover, none of the alterations appeared unique to one specific *Bbs* mutation. Although difficult to quantify, we noticed more abnormalities in epithelia that had been cultured for a longer period, a result consistent with reports of age-dependent effects in *Bbs* phenotypes (27).

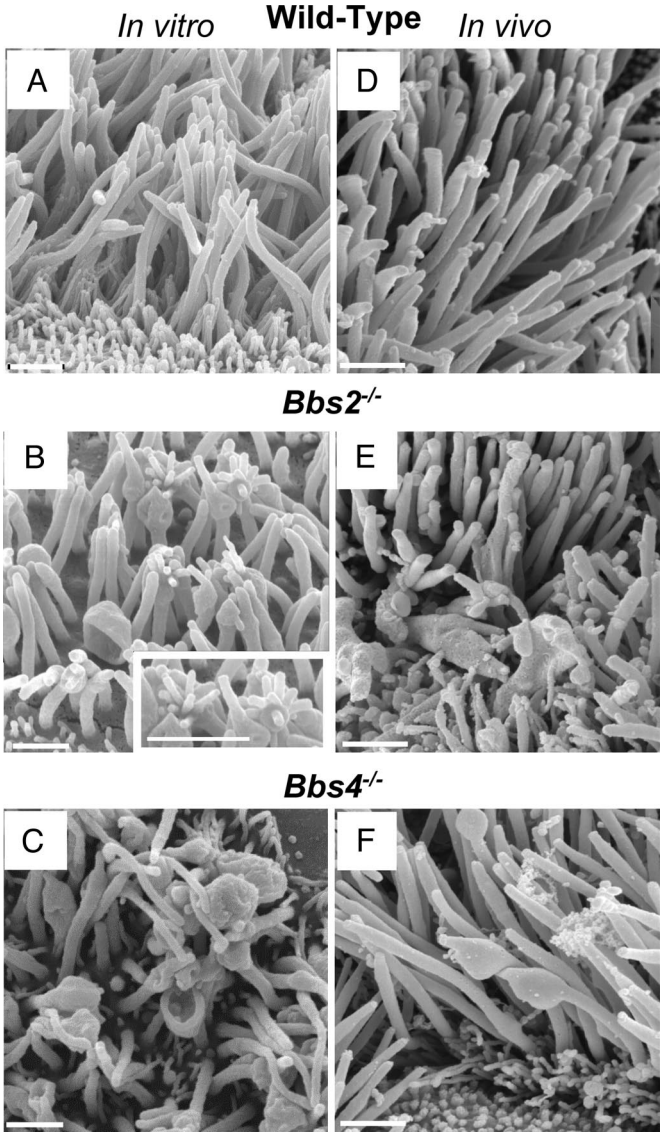

Fig. 3. Loss of BBS protein produced abnormal morphology of motile cilia. Images are SEMs of airway epithelial cultures from wild-type (*A*), *Bbs2*$^{-/-}$ (*B*), and *Bbs4*$^{-/-}$ (*C*) mice and of the *in vivo* tracheal surface from wild-type (*D*), *Bbs2*$^{-/-}$ (*E*), and *Bbs4*$^{-/-}$ (*F*) mice. *B* shows cilia with bulges at their distal end and along the shaft. Some of the cilia show sprouts at their end, giving a glove-with-fingers-like appearance; also see *Inset*. *B* and *C* also show cup-shaped cilia. SEMs from *in vivo* tissue showed similar abnormalities but less frequently. We have never observed these abnormalities in wild-type epithelia. In addition to cilia, the apical surface contains microvilli of variable number and length. (Scale bars: 1 μm.)

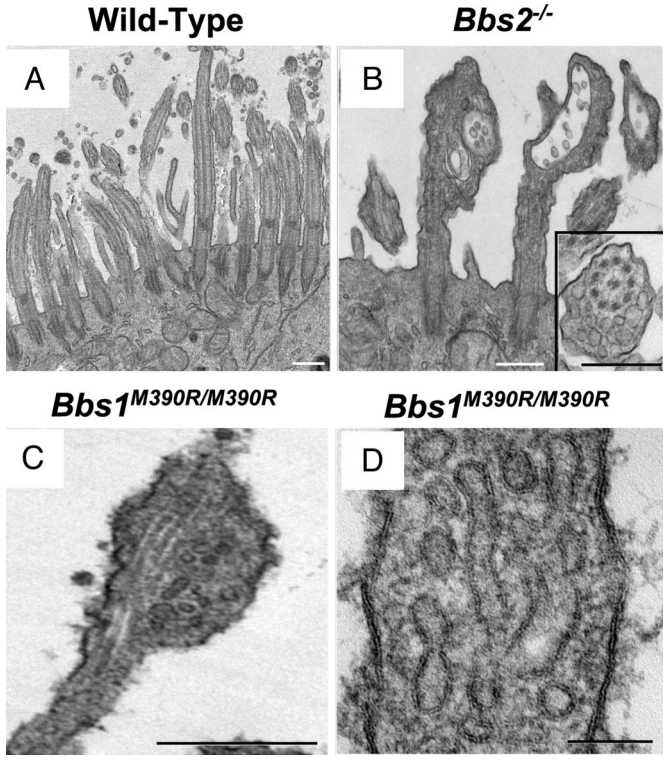

Fig. 4. Loss of BBS proteins caused a build up of vesicles in motile cilia. Data are TEM images from wild-type (*A*), *Bbs2* null (*B*), and *Bbs1* mutant (M390R) (*C* and *D*) primary cultures of differentiated airway epithelia. *B* shows bulges at the distal end of two cilia; the one on the right has a cup-like shape, and both contain vesicles. (*Inset*) Vesicles adjacent to an intact microtubule structure. *D* shows that the vesicles have a bilayer membrane. (Scale bars: *A–C*, 0.5 μm; *D*, 100 nm.)

Interestingly, in all of the *Bbs* mutants, most of the cilia appeared morphologically normal. Moreover in many cells, we detected no abnormal cilia. Thus, there was heterogeneity in the shape of the defects, heterogeneity between cilia on individual cells, and heterogeneity between different ciliated cells.

Transmission electron microscopy (TEM) also revealed abnormal ciliary morphology in all *BBS* genotypes. The most common appearance was of a bulge at the distal end of cilia, although the bulges sometimes occurred along the ciliary shaft (Fig. 4 *A–D*). Despite the misshapen appearance, the central 9 + 2 microtubule arrangement and axoneme appeared to be intact (Fig. 4 *B* and *C*). In most cases, the bulges contained vesicular structures, many of which had bilayer membranes (Fig. 4 *B–D*). In addition to the vesicular structures, the bulges contained amorphous electron-dense material. We also sometimes saw protrusions from bulges; however, because of the thin section required for TEM, we cannot be confident that they represented the sprouts observed in the SEM images.

***Bbs*-Null Mice Do Not Exhibit Increased Airway Hyperresponsiveness.** To determine whether *Bbs* mutations predispose mice to airway hyperresponsiveness, as occurs in asthma, we used an ovalbumin immunization protocol (28). Mice were systemically immunized with ovalbumin/alum and then exposed to aerosolized antigen. We then challenged them with methacholine and measured changes in airway resistance. Compared with wild-type controls, airway hyperresponsiveness was not increased in *Bbs2* or *Bbs4* null mice; in fact it decreased (Fig. 5 *A* and *B*).

As an additional assessment, we measured cells and cytokine levels in bronchoalveolar lavage liquid after ovalbumin challenge (29). The total and differential cell counts did not differ in wild-type and *Bbs*$^{-/-}$ mice (SI Fig. 10*A*). Moreover, inflammatory cytokines were not increased in either *Bbs2*$^{-/-}$ or *Bbs4*$^{-/-}$ mice (SI Fig. 10*B*). Instead, in these mice, there was a tendency for lower cytokine levels, including IL-5 and IL-13 in *Bbs2*$^{-/-}$; these cytokines are often increased in this model and in clinical asthma (29, 30). These results suggest that loss of BBS2 or BBS4 did not predispose mice to increased asthma-like responses. Indeed, there was a small protective effect.

Disruption of *Bbs* Genes Reduced Ciliary Beat Frequency. Because loss of BBS proteins altered ciliary morphology, we examined the effect on ciliary function. Respiratory cilia of *Bbs4*$^{-/-}$ and *Bbs1*

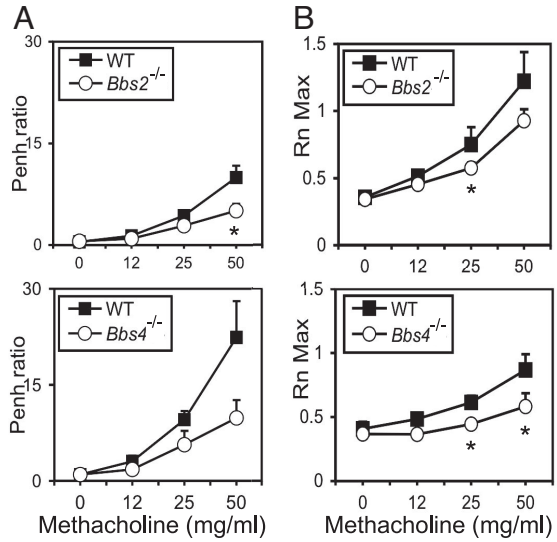

Fig. 5. *Bbs2*$^{-/-}$ and *Bbs4*$^{-/-}$ mice did not have increased airway hyperresponsiveness. Mice were immunized with ovalbumin and challenged with methacholine. We studied *Bbs2*$^{-/-}$ and *Bbs4*$^{-/-}$ mice and their wild-type littermates. Airway hyperresponsiveness was measured noninvasively by using whole-body plethysmography and recording enhanced pause (Penh) (*A*) or by using an invasive small-animal ventilator (Flexivent) (*B*). The *Bbs* mice showed reduced airway hyperresponsiveness. $n = 8$ for *Bbs2*$^{-/-}$ and wild type; $n = 6$ for *Bbs4*$^{-/-}$ and wild type. Asterisks indicate $P < 0.05$.

mutant mice retained motile activity. However, compared with wild-type, ciliary beat frequency fell (Fig. 6*A*).

To determine whether the reduced ciliary beat frequency altered mucociliary function, we measured tracheal mucociliary transport (Fig. 6*B*). Mucociliary transport was ≈100 μm/sec in wild-type animals, and it was not altered in BBS mice.

Discussion

Previous studies indicated that BBS proteins localize to primary cilia (4, 14–16). Our results show that airway epithelia, which are covered with motile cilia, express multiple *BBS* genes and at least two BBS proteins (BBS2 and BBS4) localize to cellular structures associated with motile cilia. We discovered a role for BBS proteins in motile cilia when we found structural ciliary defects in the airway epithelia of *Bbs* mutant mice. Motile cilia displayed the same misshapen appearance irrespective of whether *Bbs1*, *Bbs2*, *Bbs4*, or *Bbs6* were mutated. This result parallels the biochemical observation that the BBSome comprises each of these proteins (4).

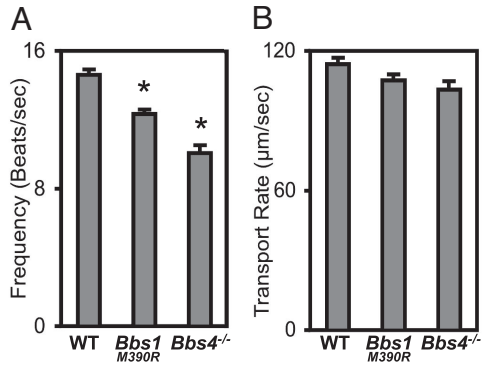

Fig. 6. Loss of BBS1 and BBS4 reduced ciliary beat frequency but did not alter mucociliary transport. (*A*) Data are ciliary beat frequency in differentiated airway epithelial cultures. $n = 8$ mice. Asterisks indicate $P < 0.001$. (*B*) Mucociliary transport rates did not significantly differ between wild-type and *Bbs* null mice. $n = 6$ mice. Data are mean ± SEM.

Clearly, the BBS proteins we studied were neither required to initiate motile ciliogenesis nor to assemble motile cilia. Instead, we speculate that they are involved in maintaining motile cilia. This suggestion is consistent with our impression that morphological deformities increased as epithelia aged in culture. It also agrees with the phenotype in BBS patients and mice where cilia form, but progressively deteriorate; an example is the photoreceptor cells that show progressive destruction over time (31, 32). The presence of motile cilia in *Bbs* airway epithelia contrasts with the absence of flagella in sperm from *Bbs* mice (9–12). The reason for the difference is not clear. However, flagella and motile cilia like those in airways do show some differences (33). Moreover, cilium-to-cilium and cell-to-cell heterogeneity in the structural abnormalities suggest that loss of BBS proteins may have subtle effects. In addition, some of the morphological variation might be due to differences in ciliary growth and turnover rates, so that not all of the cilia exhibit morphological defects at any given time.

The most striking abnormality in *Bbs* cilia was the ciliary bulges filled with vesicles. Although the mechanisms producing these changes are unknown, a defect in retrograde intraflagellar transport (IFT) may be responsible. Such a mechanism would be consistent with our finding that *Bbs* mutants left the central microtubule organization intact, that cilia formation was largely unaffected, and that bulges occurred most commonly at the tip of cilia. Moreover, external morphological abnormalities similar to those we describe result from mutations that alter the retrograde motor protein complex, including *D1bLIC*, the dynein light intermediate chain in *Chlamydomonas*, and *Dnchc2*^{lln}, a retrograde IFT motor subunit in mice (34, 35). Impaired retrograde transport of melanosomes has also been described in zebrafish upon knockdown of BBS proteins (13). An alternative explanation is that *Bbs* mutations might cause a loss of cargo from the IFT complex or abnormal cargo loading. It has been proposed that BBS proteins facilitate cargo loading at the basal body or ciliary transition zone and/or stabilize IFT-cargo interactions (15, 36). In these cases, instability of the IFT–cargo complex might lead to premature dissociation and protein buildup in the cilium. Even a small defect, magnified over time, could generate the ciliary abnormalities.

The origin of the vesicles in ciliary bulges is puzzling, especially because they are not observed in normal motile cilia. There are several possibilities. IFT proteins show homology to coat protein I and clathrin coat proteins (37, 38). Given this similarity, if IFT proteins build up in the *Bbs* cilium because of defective retrograde transport or IFT–cargo instability, they might initiate the formation of vesicles there. An alternative source of the vesicles might be from the cytoplasm. Earlier studies showed that vesicles carry transmembrane proteins from the Golgi complex to the cilium (38, 39). In addition, BBSome-associated proteins regulate Rab8, which is involved in vesicle targeting (4). Perhaps a defect in the function of the BBSome or an associated protein allows vesicles to enter the cilium.

Although previous reports suggested that patients with BBS may have an increased incidence of asthma (2, 3), the *Bbs2*$^{-/-}$ and *Bbs4*$^{-/-}$ mice displayed neither increased airway hyperresponsiveness nor substantial increases in inflammatory cytokines or cells in the ovalbumin challenge model. There are several potential explanations. First, species differences may be responsible; BBS might increase the risk for asthma in humans but not in mice. Although the ovalbumin sensitization model is widely used in asthma research, it is not identical to human asthma (40). Second, perhaps loss of BBS does predispose to "asthma" in mice, but the tests we used were not sufficiently sensitive to detect it. Third, asthma might be associated with only a subset of BBS genotypes. Although the clinical phenotype shares many

features across genotypes, precedence for variability is the observation that *Bbs4*$^{-/-}$ and *Bbs6*$^{-/-}$ mice have hypertension, whereas *Bbs2*$^{-/-}$ mice do not (ref. 10 and V.C.S., unpublished data). Fourth, because asthma is a common disease, it is possible that patients with BBS have no greater risk than the general population. Of note, pulmonary function and an in-depth validation of the asthma diagnosis have not been reported in BBS. It also seems possible that BBS caused some other pulmonary dysfunction that produced symptoms that were misinterpreted as asthma.

Our data indicate that loss of BBS2 and BBS4 partially protected mice from airway hyperresponsiveness. We speculate that this protection may have resulted from loss of a sensory function associated with either primary or motile cilia. Moreover, either airway epithelial cells or some other cells may have been responsible. Further exploration of the underlying mechanisms may provide insight into airway hyperresponsiveness and/or asthma.

In addition to the structural abnormalities, we found that *Bbs* mutations produced a functional defect, ciliary beat frequency decrease. Perhaps the misshapen cilia physically interfered with normal beating. Alternatively, loss of BBS proteins might have altered the molecular mechanism of movement in normal appearing cilia. Yet despite the reduction, mucociliary transport remained unimpaired. It seems most likely that the decrease in beat frequency was too small to significantly impact mucociliary transport. Alternatively, it is possible that our assay was not sufficiently sensitive to detect a reduction. Although it is well known that defective cilia can inhibit mucociliary transport and cause chronic airway infections and bronchiectasis (17, 19), our data are consistent with the lack of this type of lung disease in patients with BBS. It is, however, interesting that cyst-like structures within the ciliary shaft have been reported in patients with severe idiopathic bronchiectasis (41). The authors proposed that those abnormalities might cause disease, although another report suggested that the defects could be secondary to chronic airway inflammation (42). In either case, it would be interesting to know the relationship of those abnormalities to the vesicular structures we observed in cilia. In addition, it remains possible that simultaneously disrupting multiple *BBS* genes would cause more severe phenotypes.

Although most reports on BBS have focused on primary cilia, our results underscore the importance of BBS proteins in both the structure and function of motile cilia. Thus, motile cilia may be a valuable model for elucidating the molecular mechanisms involved in BBS. Moreover, additional scrutiny of the consequences of motile cilia dysfunction may be of value for patients with this disease.

Materials and Methods

For a detailed description of the materials and methods, please see *SI Text*.

Animals. Mice with disruptions of the *Bbs2*, *Bbs4*, or *Bbs6* genes or a mutation (M390R) of the *Bbs1* gene have been described (9–12).

Airway Epithelia and Cells. Primary cultures of differentiated human and mouse airway epithelia were prepared as described (21, 43). Epithelia were grown on collagen-coated filters at the air–liquid interface, where they differentiate within 14 days of seeding and develop ciliated, goblet, basal, and nonciliated columnar cells.

Adenoviruses. We used standard methods to construct adenoviruses encoding fusions of BBS2 or BBS4 with a 3xFLAG tag at the N terminus of the BBS protein.

Immunofluorescence Analysis. We used standard methods for protein immunolocalization in human airway epithelia.

Analysis of Mouse Lung. Sections of wild-type and *Bbs*$^{-/-}$ mouse lungs were stained with H&E. Cilia length from tracheal sections of wild-type (97 images from 13 mice) and *Bbs2*$^{-/-}$ (129 images from 25 mice) animals was analyzed by using NIH ImageJ software. Images were taken and analyzed in a blinded fashion.

Electron Microscopy. For SEM and TEM, we used standard methods to study cultured epithelia or *in vivo* mouse trachea.

Assessment of Airway Hyperresponsiveness. Mice were sensitized by i.p. injection of 10 μg ovalbumin mixed with 1 mg of alum at days 0 and 7. Mice were then challenged with inhaled OVA (1% solution, 30 min) on days 14 and 16. Airway hyperresponsiveness to inhaled methacholine was measured by using whole-body plethysmography as described (29). Responses were measured by using the enhanced pause (Penh). We also measured central airway resistance (Rn) in OVA-challenged mice (44). After euthanasia, bronchoalveolar lavage was prepared for cell counts and measurement of cytokine and chemokine concentrations.

Ciliary Beat Frequency. Line scans of cilia movement in mouse airway epithelia were collected at 2-ms intervals (2,000 lines collected over 4 sec). Data were analyzed by using NIH ImageJ software.

Mucociliary Transport. For these measurements, a window was made in the upper trachea, and yellow fluorescent 1-μm spheres were deposited on the trachea. Sequential images were obtained with a dissecting stereoscope by scanning every 0.5 sec for 60 sec. Distances that particles moved were calculated by using NIH ImageJ software. Experiments were conducted blinded to genotype.

ACKNOWLEDGMENTS. We thank Phil Karp, Tami Nesselhauf, and Theresa Mayhew for excellent assistance. We appreciate valuable assistance from the University of Iowa *In Vitro* Models and Cell Culture Core, the Gene Transfer Vector Core, the Morphology Core and the Central Microscopy Research Facility, all supported in part by the National Institutes of Health (NIH) Grants HL51670, HL61234, and DK54759 and the Cystic Fibrosis Foundation. This work was supported in part by NIH Grants HL59324 and DE014390. V.C.S. and M.J.W. are Investigators of the Howard Hughes Medical Institute.

1. Mykytyn K, Sheffield VC (2004) Establishing a connection between cilia and Bardet–Biedl syndrome. *Trends Mol Med* 10:106–109.
2. Beales PL, Elcioglu N, Woolf AS, Parker D, Flinter FA (1999) New criteria for improved diagnosis of Bardet–Biedl syndrome: Results of a population survey. *J Med Genet* 36:437–446.
3. Moore SJ, *et al.* (2005) Clinical and genetic epidemiology of Bardet–Biedl syndrome in Newfoundland: A 22-year prospective, population-based, cohort study. *Am J Med Genet A* 132:352–360.
4. Nachury MV, *et al.* (2007) A core complex of BBS proteins cooperates with the GTPase Rab8 to promote ciliary membrane biogenesis. *Cell* 129:1201–1213.
5. Tobin JL, Beales PL (2007) Bardet–Biedl syndrome: Beyond the cilium. *Pediatr Nephrol* 22:926–936.
6. Li JB, *et al.* (2004) Comparative genomics identifies a flagellar and basal body proteome that includes the BBS5 human disease gene. *Cell* 117:541–552.
7. Chiang AP, *et al.* (2004) Comparative genomic analysis identifies an ADP-ribosylation factor-like gene as the cause of Bardet–Biedl syndrome (BBS3). *Am J Hum Genet* 75:475–484.
8. Avidor-Reiss T, *et al.* (2004) Decoding cilia function: Defining specialized genes required for compartmentalized cilia biogenesis. *Cell* 117:527–539.
9. Mykytyn K, *et al.* (2004) Bardet–Biedl syndrome type 4 (BBS4)-null mice implicate Bbs4 in flagella formation but not global cilia assembly. *Proc Natl Acad Sci USA* 101:8664–8669.
10. Nishimura DY, *et al.* (2004) Bbs2-null mice have neurosensory deficits, a defect in social dominance, and retinopathy associated with mislocalization of rhodopsin. *Proc Natl Acad Sci USA* 101:16588–16593.
11. Fath MA, *et al.* (2005) Mkks-null mice have a phenotype resembling Bardet–Biedl syndrome. *Hum Mol Genet* 14:1109–1118.
12. Davis RE, *et al.* (2007) A knockin mouse model of the Bardet–Biedl syndrome 1 M390R mutation has cilia defects, ventriculomegaly, retinopathy, and obesity. *Proc Natl Acad Sci USA* 104:19422–19427.
13. Yen HJ, *et al.* (2006) Bardet–Biedl syndrome genes are important in retrograde intracellular trafficking and Kupffer's vesicle cilia function. *Hum Mol Genet* 15:667–677.
14. Ansley SJ, *et al.* (2003) Basal body dysfunction is a likely cause of pleiotropic Bardet–Biedl syndrome. *Nature* 425:628–633.
15. Blacque OE, *et al.* (2004) Loss of *C. elegans* BBS-7 and BBS-8 protein function results in cilia defects and compromised intraflagellar transport. *Genes Dev* 18:1630–1642.
16. Kim JC, *et al.* (2004) The Bardet–Biedl protein BBS4 targets cargo to the pericentriolar region and is required for microtubule anchoring and cell cycle progression. *Nat Genet* 36:462–470.
17. Pan J, Wang Q, Snell WJ (2005) Cilium-generated signaling and cilia-related disorders. *Lab Invest* 85:452–463.
18. Pedersen LB, Geimer S, Rosenbaum JL (2006) Dissecting the molecular mechanisms of intraflagellar transport in chlamydomonas. *Curr Biol* 16:450–459.

19. Fliegauf M, Benzing T, Omran H (2007) When cilia go bad: Cilia defects and ciliopathies. *Nat Rev Mol Cell Biol* 8:880–893.
20. Kulaga HM, *et al.* (2004) Loss of BBS proteins causes anosmia in humans and defects in olfactory cilia structure and function in the mouse. *Nat Genet* 36:994–998.
21. Karp PH, *et al.* (2002) in *Epithelial Cell Culture Protocols*, ed Wise C (Humana, Totowa, NJ), pp 115–137.
22. You Y, Richer EJ, Huang T, Brody SL (2002) Growth and differentiation of mouse tracheal epithelial cells: Selection of a proliferative population. *Am J Physiol* 283:L1315–L3121.
23. Kim JC, *et al.* (2005) MKKS/BBS6, a divergent chaperonin-like protein linked to the obesity disorder Bardet–Biedl syndrome, is a novel centrosomal component required for cytokinesis. *J Cell Sci* 118:1007–1020.
24. Jurczyk A, *et al.* (2004) Pericentrin forms a complex with intraflagellar transport proteins and polycystin-2 and is required for primary cilia assembly. *J Cell Biol* 166:637–643.
25. Pazour GJ, *et al.* (2000) Chlamydomonas IFT88 and its mouse homologue, polycystic kidney disease gene tg737, are required for assembly of cilia and flagella. *J Cell Biol* 151:709–718.
26. Mokrzan EM, Lewis JS, Mykytyn K (2007) Differences in renal tubule primary cilia length in a mouse model of Bardet–Biedl syndrome. *Nephron Exp Nephrol* 106:e88–e96.
27. Eichers ER, *et al.* (2006) Phenotypic characterization of Bbs4 null mice reveals age-dependent penetrance and variable expressivity. *Hum Genet* 120:211–226.
28. Jain VV, *et al.* (2002) CpG-oligodeoxynucleotides inhibit airway remodeling in a murine model of chronic asthma. *J Allergy Clin Immunol* 110:867–872.
29. Kline JN, Kitagaki K, Businga TR, Jain VV (2002) Treatment of established asthma in a murine model using CpG oligodeoxynucleotides. *Am J Physiol* 283:L170–L179.
30. Zhu Z, *et al.* (1999) Pulmonary expression of interleukin-13 causes inflammation, mucus hypersecretion, subepithelial fibrosis, physiologic abnormalities, and eotaxin production. *J Clin Invest* 103:779–788.
31. Azari AA, *et al.* (2006) Retinal disease expression in Bardet–Biedl syndrome-1 (BBS1) is a spectrum from maculopathy to retina-wide degeneration. *Invest Ophthalmol Vis Sci* 47:5004–5010.
32. Swiderski RE, *et al.* (2007) Gene expression analysis of photoreceptor cell loss in bbs4-knockout mice reveals an early stress gene response and photoreceptor cell damage. *Invest Ophthalmol Vis Sci* 48:3329–3340.
33. Dawe HR, Farr H, Gull K (2007) Centriole/basal body morphogenesis and migration during ciliogenesis in animal cells. *J Cell Sci* 120:7–15.
34. Hou Y, Pazour GJ, Witman GB (2004) A dynein light intermediate chain, D1bLIC, is required for retrograde intraflagellar transport. *Mol Biol Cell* 15:4382–4394.
35. Huangfu D, Anderson KV (2005) Cilia and Hedgehog responsiveness in the mouse. *Proc Natl Acad Sci USA* 102:11325–11330.
36. Blacque OE, Cevik S, Kaplan OI (2008) Intraflagellar transport: From molecular characterisation to mechanism. *Front Biosci* 13:2633–2652.
37. Jekely G, Arendt D (2006) Evolution of intraflagellar transport from coated vesicles and autogenous origin of the eukaryotic cilium. *BioEssays* 28:191–198.
38. Reiter JF, Mostov K (2006) Vesicle transport, cilium formation, and membrane specialization: The origins of a sensory organelle. *Proc Natl Acad Sci USA* 103:18383–18384.
39. Wang S, Luo Y, Wilson PD, Witman GB, Zhou J (2004) The autosomal recessive polycystic kidney disease protein is localized to primary cilia, with concentration in the basal body area. *J Am Soc Nephrol* 15:592–602.
40. Zosky GR, *et al.* (2007) Ovalbumin-sensitized mice are good models for airway hyperresponsiveness but not acute physiological responses to allergen inhalation. *Clin Exp Allergy*, PMID: 18070158.
41. Tsang KW, *et al.* (2000) Severe bronchiectasis in patients with ''cystlike'' structures within the ciliary shafts. *Am J Respir Crit Care Med* 161:1300–1305.
42. Pifferi M, *et al.* (2004) ''Cyst-like'' structures within the ciliary shafts in children with bronchiectasis. *Eur Respir J* 23:857–860.
43. You Y, *et al.* (2004) Role of f-box factor foxj1 in differentiation of ciliated airway epithelial cells. *Am J Physiol* 286:L650–L657.
44. Kitagaki K, *et al.* (2006) Intestinal helminths protect in a murine model of asthma. *J Immunol* 177:1628–1635.
45. Piperno G, Fuller MT (1985) Monoclonal antibodies specific for an acetylated form of alpha-tubulin recognize the antigen in cilia and flagella from a variety of organisms. *J Cell Biol* 101:2085–2094.